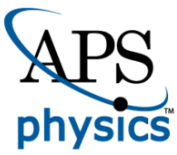

Viscous Dissipation and Heat Conduction in Binary Neutron-Star Mergers

Mark G. Alford, Luke Bovard, Matthias Hanauske, Luciano Rezzolla, and Kai Schwenzer

Phys. Rev. Lett. **120**, 041101 — Published 23 January 2018

DOI: 10.1103/PhysRevLett.120.041101

On the importance of viscous dissipation and heat conduction in binary neutron-star mergers

Mark G. Alford,[1] Luke Bovard,[2] Matthias Hanauske,[2,3] Luciano Rezzolla,[2,3] and Kai Schwenzer[4,5]

[1]*Physics Department, Washington University, St. Louis, MO 63130, USA*
[2]*Institut für Theoretische Physik, Max-von-Laue-Strasse 1, 60438 Frankfurt, Germany*
[3]*Frankfurt Institute for Advanced Studies, Ruth-Moufang-Strasse 1, 60438 Frankfurt, Germany*
[4]*Theoretical Astrophysics (IAAT), Eberhard Karls University of Tübingen, Tübingen 72076, Germany*
[5]*Department of Astronomy and Space Sciences, Istanbul University, Beyazıt, 34119, Istanbul, Turkey*

Inferring the properties of dense matter is one of the most exciting prospects from the measurement of gravitational waves from neutron star mergers. However, it requires reliable numerical simulations that incorporate viscous dissipation and energy transport as these can play a significant role in the survival time of the post-merger object. We calculate timescales for typical forms of dissipation and find that thermal transport and shear viscosity will not be important unless neutrino trapping occurs, which requires temperatures above 10 MeV and gradients over lengthscales of 0.1 km or less. On the other hand, if direct-Urca processes remain suppressed, leaving modified-Urca processes to establish flavor equilibrium, then bulk viscous dissipation could provide significant damping to density oscillations right after merger. When comparing with data from state-of-the-art merger simulations, we find that the bulk viscosity takes values close to its resonant maximum in a typical merger, motivating a more careful assessment of the role of bulk viscous dissipation in the gravitational-wave signal from merging neutron stars.

PACS numbers:

Introduction. The recent discovery of a binary neutron star merger both across nearly the entire electromagnetic spectrum [1] and in gravitational waves [2]—not even two years after their first detection by LIGO in black-hole mergers [3]—as well as the striking confirmation of such mergers as the central engine of short gamma-ray bursts (see [4, 5] for reviews) heralds the era of gravitational wave astronomy. Detailed observations of such events could provide valuable information about the properties of matter at extreme density and temperature. With a few exceptions [6, 7] current simulations of neutron-star mergers neglect the transport properties of the material, assuming that they are too small to operate on dynamical timescales [8]. We revisit this assumption by exploring the impact of viscosity and thermal transport after merger, exploiting results of simulations. These have seen enormous progress [9–13] and found that for not too massive or too asymmetric systems, the post-merger object is metastable to gravitational collapse over tens of milliseconds. The inner region of this object, $\sim 10\,\mathrm{km}$ across, can reach several times nuclear-matter saturation (number) density $n_0 \approx 0.16\,\mathrm{fm}^{-3}$ and temperatures of tens of MeV.

The details of the complicated post-merger phase depend on the mass of the system, the equation of state (EOS), and the magnetic fields that develop after the merger [4, 5]. Quite generically, unless it collapses promptly to a black hole [10], the binary-merger product will oscillate in modes that leave a clear imprint on the gravitational-wave signal [14–18]. In such simulations, the large scale motion is damped mostly by gravitational-wave emission over tens of milliseconds. This sets the timescale over which dissipation or transport processes would have to operate to influence the gravitational-wave or neutrino signal. These dynamical processes depend on the low energy degrees of freedom and can vary dramatically between different phases, offering the possibility of using merger data to probe the phase structure of dense matter, potentially including exotic phases such as quark matter, despite the significant uncertainties in the post-merger dynamics. In this *Letter* we provide estimates of the timescales of transport and dissipation processes for a typical post-merger scenario.

Thermal equilibration. To establish whether heat diffusion is significant, consider a region of size $z_{\rm typ}$ that is hotter than its surroundings by a temperature difference ΔT. For a material with specific heat per unit volume c_V and thermal conductivity κ, this region has an additional thermal energy $E_{\rm th} \approx (\pi/6) c_V z_{\rm typ}^3 \Delta T$ and (assuming a smooth temperature distribution so that the thermal gradient is $\Delta T/z_{\rm typ}$) heat is conducted out of the region at a rate $W_{\rm th} \approx \pi \kappa \Delta T z_{\rm typ}$. The thermal equilibration time, needed to conduct away a significant fraction of the extra thermal energy, is $\tau_\kappa \equiv E_{\rm th}/W_{\rm th} = c_V z_{\rm typ}^2/(6\kappa)$. The specific heat is dominated by neutrons, which have the largest phase space of low-energy excitations, giving $c_V \approx 1.0\, m_n^* n_n^{1/3} T$, assuming a Fermi liquid of neutron density n_n with Landau effective mass m_n^* [19]. Particles of number density n_i, typical speed v_i, and mean free path (mfp) λ_i, contribute to the thermal conductivity as $\kappa \propto \sum_i \kappa_i \propto \sum_i n_i v_i \lambda_i$, so κ is effectively dominated by particles with the optimal combination of high density and long mfp. Neutrons, though numerous, are strongly interacting and have a very short mfp, thus thermal conductivity is dominated by electrons or neutrinos.

Below a few MeV, the neutrino mfp becomes longer than the merger region [4, 20], so neutrinos escape and thermal conductivity is dominated by electrons which scatter mainly via exchange of Landau-damped transverse photons. In this approximation, the thermal conductivity is temperature-independent $\kappa_e \approx 1.5\, n_e^{2/3}/\alpha$ [Eq. (40) of [21]], where n_e is the electron number density and $\alpha \approx 1/137$. This yields a lower bound for the thermal equilibration time in the electron

dominated regime

$$\tau_\kappa^{(e)} = 5\times10^8\,\mathrm{s} \times \left(\frac{0.1}{x_p}\right)^{\frac{2}{3}} \left(\frac{m_n^*}{0.8\,m_n}\right) \left(\frac{n_0}{n_{_B}}\right)^{\frac{1}{3}} \left(\frac{z_{\rm typ}}{1\,\mathrm{km}}\right)^2 \left(\frac{T}{1\,\mathrm{MeV}}\right), \quad (1)$$

where $n_{_B}$ is the baryon number density, n_0 nuclear saturation density and $x_p \equiv n_e/n_{_B}$ is the proton fraction. Clearly, this timescale is far too large to have an impact on the $\sim 10\,$ms timescale of post-merger processes [4].

At temperatures $T \gtrsim 10$ MeV, neutrinos become trapped for nucleon density $n \gtrsim n_0$, since the neutrino mfp, which at high density depends strongly on in-medium corrections [20, 22], becomes smaller than the star. Electron neutrinos form a degenerate Fermi gas with a Fermi momentum $p_{F,\nu}$ of about half that of the electrons. Their mfp is longer than that of the electrons, so they dominate the thermal conductivity [23], which is given by $\kappa_\nu \approx 0.33\, n_\nu^{2/3}/(G_F^2 (m_n^*)^2 n_e^{1/3} T)$, where $G_F \equiv 1/(293\,\mathrm{MeV})^2$ is the Fermi coupling. This yields the timescale for thermal transport via neutrinos

$$\tau_\kappa^{(\nu)} \approx 0.7\,\mathrm{s} \times \left(\frac{0.1}{x_p}\right)^{\frac{1}{3}} \left(\frac{m_n^*}{0.8\,m_n}\right)^3 \left(\frac{\mu_e}{2\,\mu_\nu}\right)^2 \left(\frac{z_{\rm typ}}{1\,\mathrm{km}}\right)^2 \left(\frac{T}{10\,\mathrm{MeV}}\right)^2. \quad (2)$$

In summary, for neutrino-driven thermal transport to be important on a timescale of tens of milliseconds, there would e.g. have to be thermal gradients (e.g., from turbulence) on lengthscales of the order 0.1 km. Moreover, heat transport into cooler regions should manifest itself even more quickly.

Shear dissipation. To estimate the shear-viscosity timescale, consider a fluid of rest-mass density ρ flowing in the x direction at velocity v_x, having kinetic energy per unit volume $E_{\rm kin} = \frac{1}{2}\rho v_x^2$. If the fluid has shear viscosity η, then the energy dissipated per unit time and unit volume is $W_{\rm shear} \approx \eta (dv_x/dz)^2$, and the time needed for shear viscosity to dissipate a significant fraction of the kinetic energy is $\tau_\eta \equiv E_{\rm kin}/W_{\rm shear}$. We assume that the flow is fairly uniform, with the velocity varying by a factor of order unity over a distance $z_{\rm typ}$ in the z direction, so $dv_x/dz \approx v_x/z_{\rm typ}$ which gives $\tau_\eta \approx \rho\, z_{\rm typ}^2/(2\eta)$.

In the low-temperature, electron-dominated regime ($T \lesssim 10\,\mathrm{MeV}$), using the dominant transverse contribution from [24] [Eq. (2.4) in [25]] with the damping scale $q_t^2 \equiv 4\alpha p_{F,e}^2/\pi$, we find $\eta^{(e)} \approx 0.2\, n_e^{14/9}/(\alpha^{5/3}\, T^{5/3})$, so

$$\tau_\eta^{(e)} \approx 1.6{\times}10^8\,\mathrm{s} \left(\frac{z_{\rm typ}}{1\,\mathrm{km}}\right)^2 \left(\frac{T}{1\,\mathrm{MeV}}\right)^{\frac{5}{3}} \left(\frac{n_0}{n_{_B}}\right)^{\frac{5}{9}} \left(\frac{0.1}{x_p}\right)^{\frac{14}{9}}, \quad (3)$$

again being far too large to be relevant.

However, in the high-temperature, neutrino-dominated regime ($T \gtrsim 10\,\mathrm{MeV}$) neutrinos produce a much larger shear viscosity $\eta^{(\nu)} \approx 0.46\, n_\nu^{4/3} / \left(G_F^2 (m_n^*)^2 n_e^{1/3} T^2\right)$ [23], which yields

$$\tau_\eta^{(\nu)} \approx 54\,\mathrm{s} \left(\frac{0.1}{x_p}\right) \left(\frac{m_n^*}{0.8\,m_n}\right)^2 \left(\frac{\mu_e}{2\,\mu_\nu}\right)^4 \left(\frac{z_{\rm typ}}{1\,\mathrm{km}}\right)^2 \left(\frac{T}{10\,\mathrm{MeV}}\right)^2, \quad (4)$$

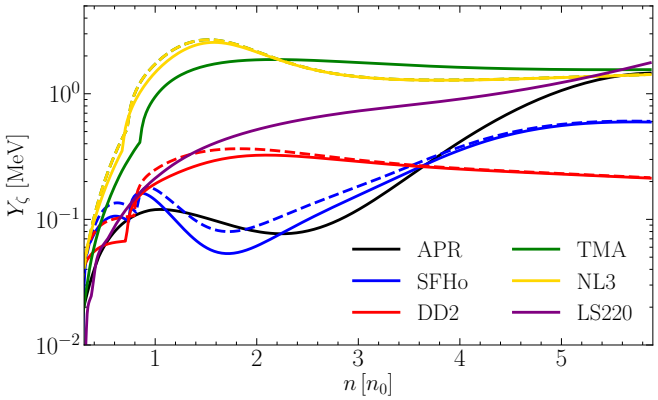

Figure 1: Density dependence of the maximum-bulk-viscosity prefactor Y_ζ [Eq. (5)] for various EOSs. Solid lines are for cold matter ($T = 0.1\,$MeV) while dashed lines are for hot matter ($T = 10\,$MeV). For LS220 we only give a single curve at $T = 1\,$MeV, due to numerical issues in the EOS table.

Interestingly, like eq. (2), this result depends only weakly on the density, via the proton fraction x_p, the effective mass m_n^* and the ratio μ_e/μ_ν. In summary, neutrino shear viscosity could play an important role, i.e., $\tau_\eta^{(\nu)}$ could be in the millisecond range, if the neutrino density is anomalously high or if there are flows that experience shear over short distances, $z_{\rm typ} \sim 0.01\,$km, for example, due to turbulence or high-order non-axisymmetric instabilities [26–29].

Bulk viscosity. To study the impact of bulk viscosity, we consider an "averaged" bulk viscosity $\bar\zeta$ in response to a periodic compression-rarefaction cycle. In nuclear matter, dissipation arises because the rate of beta equilibration of the proton fraction via Urca processes occurs on the same timescale, so that the proton fraction lags behind the applied pressure. If the oscillations after the merger are roughly periodic, we expect that the dissipation induced by pressure variations occurring on a timescale $t_{\rm dens}$ can be estimated by using the bulk viscosity evaluated at frequency $f = 1/t_{\rm dens}$. The bulk viscosity is largest when the internal equilibration rate matches the frequency of the oscillation. Furthermore, because the equilibration rate is sensitive to the temperature, the bulk viscosity shows a resonant maximum as a function of temperature (e.g., Fig. 7 in [30]). For oscillations with a timescale $t_{\rm dens}$, the resonant maximum value is [30]

$$\bar\zeta_{\rm max} \equiv Y_\zeta\, \bar n\, t_{\rm dens}\,, \qquad Y_\zeta \equiv C^2/(4\pi B \bar n)\,, \quad (5)$$

where $B \equiv -(1/\bar n)\,(\partial\delta\mu/\partial x_p)|_n$ and $C \equiv \bar n\,(\partial\delta\mu/\partial n)|_{x_p}$ are the nuclear susceptibilities with respect to baryon density and proton fraction, where the chemical potential $\delta\mu \equiv \mu_n - \mu_p - \mu_e$ characterises, in the absence of neutrino trapping, the degree to which the system is out of beta equilibrium. This maximum value $\bar\zeta_{\rm max}$ depends only on properties of the EOS and is *independent* of the flavor re-equilibration rate. Changing the re-equilibration rate moves the curve in Fig. 7 in [30] "horizontally", changing the temperature at which the maximum value is attained.

We note that the maximum bulk viscosity is a monotoni-

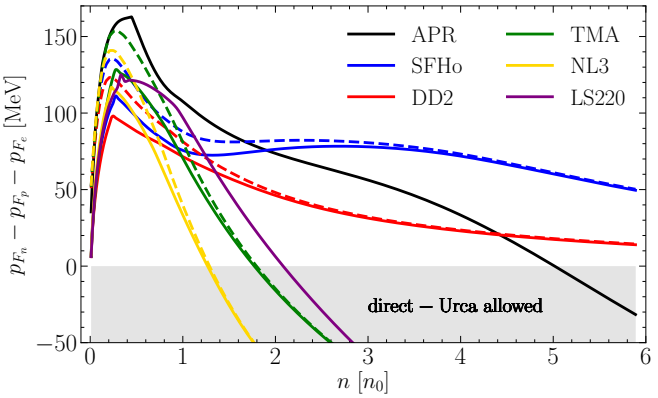

Figure 2: Momentum difference relevant to the direct-Urca channel as a function of density, for the EOSs shown in Fig. 1. For negative values, direct-Urca processes are allowed (gray-shaded area).

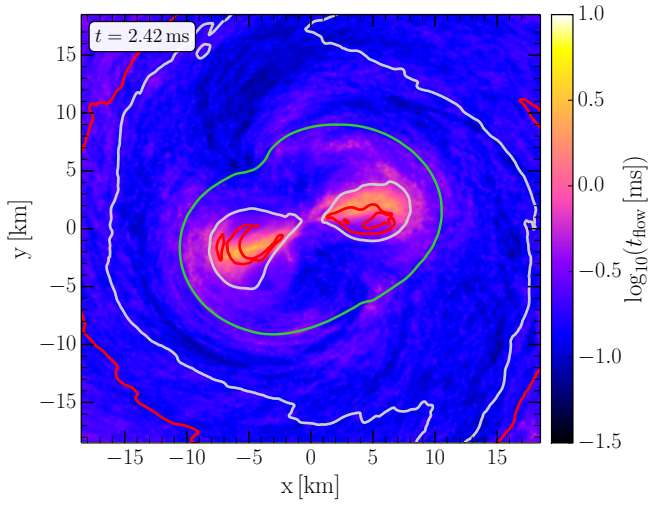

Figure 3: The flow timescale $t_{\rm flow}$ obtained from a numerical-relativity simulation of two $1.35\,M_\odot$ neutron stars [39]. The red (4 MeV) and gray (7 MeV) contours show the boundaries of the temperature range in which the bulk viscosity roughly takes its maximum value, while the green contour shows the inner region where the rest-mass density exceeds nuclear saturation density.

cally increasing function of number density and Fig. 1 shows the prefactor Y_ζ for nuclear matter obeying various EOSs, all of which can sustain a $2\,M_\odot$ neutron star [31, 32]. Whereas APR [33] is a cold EOS and is included here for comparison, for all the others we use "hot" EOSs calculated using a model of nuclei and interacting nucleons in statistical equilibrium [34]. In addition to the LS220 [35], used for the simulations below, these EOSs range from the moderately soft SHFo [36] through the increasingly stiff DD2 [36, 37] and TMA [34], to the extremely stiff NL3.

Now consider the temperature $T_{\zeta\max}$ at which bulk viscosity reaches its resonant maximum. For small-amplitude oscillations $T_{\zeta\max} = (2\pi\, f/(\tilde{\Gamma}B))^{1/\delta}$ [30], where $\tilde{\Gamma}$ is the prefactor in the equilibration rate, $\Gamma = \tilde{\Gamma} T^\delta \delta\mu$. For modified-Urca processes, $\delta = 6$, so $1/\delta$ is small, making $T_{\zeta\max}$ insensitive to details of the EOS. As a result, over the enire relevant frequency range, i.e., from a few tenths to several kHz, we find for flavor equilibration via nuclear modified-Urca "nmU" processes

$$T_{\zeta\max}^{\rm nmU} \approx 4 - 7\,{\rm MeV} \approx 5 - 8\times 10^{10}\,{\rm K}\,, \qquad (6)$$

which is well within the range of temperatures expected for dense matter in the post-merger [4, 38, 39].

It should be noted that flavor re-equilibration might instead occur via direct-Urca reactions, which are orders of magnitude faster than modified-Urca processes, giving much lower bulk viscosities at $T \sim 5\,{\rm MeV}$, since the resonant maximum of bulk viscosity would have moved to lower temperatures (Fig. 7 in [30]). In neutrino-transparent matter at $T = 0$, direct-Urca processes are allowed when $\Delta p_F \equiv p_{F,n} - p_{F,p} - p_{F,e} < 0$. In Fig. 2 we plot this kinematic constraint as a function of density for the same EOSs in Fig. 1. For softer EOSs (e.g., SFHo, DD2) direct-Urca processes are never possible at $T = 0$; however, for APR the direct-Urca channel opens at $n > 5\,n_0$. For even stiffer EOSs (LS220, NL3, TMA) it already opens around twice saturation density, yet these EOSs have been challenged by nuclear physics constraints [40]. These considerations suggest that the amount of bulk-viscous damping will be a sensitive indicator of whether the EOS allows direct Urca processes at the densities and temperatures prevalent in neutron star mergers. A more precise connection with the EOS will require calculations of the beta equilibration rate that incorporate the effects of temperature, strong interactions, and the gradual opening of phase space above the direct Urca threshold.

We now estimate the dissipation time for compression oscillations. The energy density for a baryon number-density oscillation of amplitude Δn around average density $\bar{n}$ is $\mathcal{E}_{\rm comp} \approx K\bar{n}(\Delta n/\bar{n})^2/18$ [41], where K is the nuclear compressibility at that density. If the compression varies on a timescale $t_{\rm dens}$, then, in a material with bulk viscosity $\bar{\zeta}$, the dissipated power per unit volume is [42] $(d\mathcal{E}/dt)_{\rm bulk} \approx 2\pi^2\bar{\zeta}\,(\Delta n/\bar{n})^2\,/t_{\rm dens}^2$. Hence, the time required for bulk viscosity to have a significant impact on the oscillations of the system is

$$\tau_\zeta \equiv \mathcal{E}_{\rm comp}/\,(d\mathcal{E}/dt)_{\rm bulk} \approx K\bar{n}\,t_{\rm dens}^2/(36\pi^2\,\bar{\zeta})\,. \qquad (7)$$

Expecting bulk viscosity to reach its maximum value $\bar{\zeta}_{\rm max}$ [Eq. (5)] at typical neutron-star merger temperatures [Eq. (6)], we can use Eq. (5) in (7) to find that, when the direct-Urca channel is not open, the minimum timescale for bulk viscosity to impact the oscillations is

$$\tau_\zeta^{\rm min} \approx 3\,{\rm ms}\left(\frac{t_{\rm dens}}{1\,{\rm ms}}\right)\left(\frac{K}{250\,{\rm MeV}}\right)\left(\frac{0.25\,{\rm MeV}}{Y_\zeta}\right)\,. \qquad (8)$$

Stated differently, under conditions of maximum bulk viscosity, the damping timescale is a few times larger than the typical timescale $t_{\rm dens}$ of density variations.

Since strong emission of gravitational waves occurs from the high-density region of the star during the first $\sim$ 5 milliseconds after the merger, when characteristic frequencies f_1

and f_3 appear in the gravitational-wave spectrum [16, 18, 43], bulk viscous damping is most likely to have observable consequences if, during that early time, there are density oscillations occurring on a millisecond timescale in parts of the high-density region where the bulk viscosity is maximal ($T \sim 4-7\,\mathrm{MeV}$).

To test whether such conditions are met, we show in Figs. 3 and 4 results from a state-of-the-art simulation of a symmetric merger of $M = 2 \times 1.35\,M_\odot$, consistent with GW170817 [2], using the LS220 EOS [35], where $t = 0$ is the time of merger [43]. Figure 3 uses a colorcode to show the expansion flow timescale $t_{\rm flow} \equiv 1/\langle|\vec{\nabla}\cdot\vec{v}|\rangle = \rho/D_t\rho$ where $\langle\ \rangle$ represents a time average over a 2 ms time window and where D_t is the Lagrangian time derivative in Newtonian hydrodynamics [44]. This quantity is easily measured and, for a harmonic density oscillation, it is related to Eqs. (7) and (8) by $t_{\rm dens} \approx (4\Delta n/\bar{n})t_{\rm flow}$. Figure 3 reports $t_{\rm flow}$ 2.4 ms after the merger, where the post-merger object is in its violent and shock-dominated transient phase, (see [43] for a toy model of this phase). Inside the green contour, the rest-mass density is above nuclear saturation. The red and gray lines are temperature contours at 4 MeV and 7 MeV, respectively. Overall, Fig. 3 shows that there are significant regions where Eq. (8) is a valid estimate of the dissipation time because the density is high and the temperature is in the range that maximizes bulk viscosity [Eq. (6)]. Since in these regions $t_{\rm flow} \sim 0.1 - 1\,\mathrm{ms}$ and $\Delta n/\bar{n} \sim 1$, we conclude that $t_{\rm dens} \approx (4\Delta n/\bar{n})t_{\rm flow} \sim t_{\rm flow}$, is indeed in the millisecond range.

This conclusion is reinforced by Fig. 4, which shows the evolution of various local properties of representative tracer particles in the inner region of the merger product [45]. From the top panel, which reports the evolution of the temperature, we see that all tracers pass through the temperature range of large bulk viscosity (dark and light-gray shaded areas, showing the regions of maximum and up to an order of magnitude smaller dissipation) during the first few milliseconds. The second panel reports the evolution of the normalized rest-mass density and shows that at early times ($t \lesssim 5\,\mathrm{ms}$) there are variations of order 100% in the rest-mass density on a timescale of milliseconds, confirming that $t_{\rm dens}$ is in that range. The third panel shows the average of $t_{\rm flow}$ for the tracers, which is in the $0.1 - 1\,\mathrm{ms}$ range, as expected from Fig. 3. Finally, the bottom panel of Fig. 4 is a spectrogram averaging the power spectral densities of the normalized rest-mass densities in the second panel and showing how, throughout the first 20 ms, the merger product has oscillation with a significant power at frequencies in the kHz range.

The results shown in Figs. 3 and Fig. 4, combined with Eq. (8), suggest that if direct Urca processes remain suppressed, then significant bulk viscous dissipation may occur on timescales of a few milliseconds, which is fast enough to affect the flow of nuclear material, and hence the emitted gravitational signal. Full numerical-relativity simulations accounting for bulk viscosity are necessary to quantify the amount of such dissipation and its impact on the gravitational-wave signal.

Conclusions. Material properties can only play a significant role in neutron-star mergers if the relevant dissipation time is comparable with or shorter than the survival time of the post-merger object. Using typical values found in numerical simulations, we find that shear viscosity and thermal conductivity are not likely to play a major role in post-merger dynamics unless neutrino trapping occurs, which requires $T \gtrsim 10\,\mathrm{MeV}$, and $z_{\rm typ} \lesssim 0.01\,\mathrm{km}$. On the other hand, if direct-Urca processes remain suppressed, leaving modified-Urca processes to establish flavor equilibrium, then bulk viscous dissipation could provide significant damping of the high-amplitude density oscillations observed right after merger. We conclude that viscous dissipative processes deserve more careful investigation since they may well affect the spectral properties of the post-merger gravitational-wave signal, especially the f_1 and f_3 peaks that are produced right after the merger and that are dissipated rapidly [14–16, 18, 46]. Since these peaks are routinely employed to infer the properties of the EOS [47, 48], a more realistic treatment is particularly important. In addition, if viscous dissipation is active after the merger, it will also heat the merger product, possibly stabilizing it on longer timescales via the extra thermal pressure [10, 49–51]. If future gravitational-wave observations indicate that the actual dissipation is much smaller than what is suggested by Eq. (8),

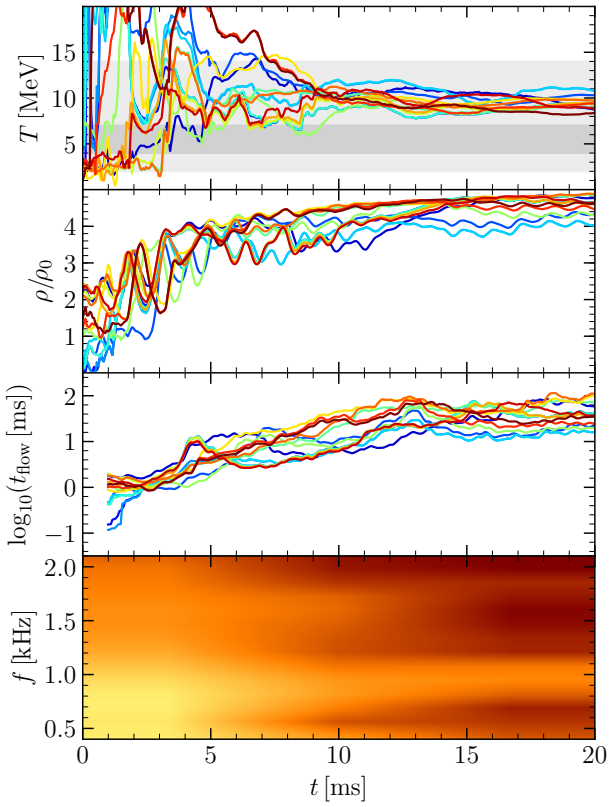

Figure 4: Co-moving time variation of physical properties of post-merger material from selected tracers in the same merger as shown in Fig. 3. Top panel: temperature [the shaded regions are where bulk viscosity is large, see Eq. (6)]. Second panel: rest-mass density. Third panel: flow timescale $t_{\rm flow}$. Bottom panel: spectrogram averaging the rest-mass density evolutions in the second panel.

e.g. if merger material transforms to quark matter, this would put limits on the fraction of matter for which direct-Urca processes are suppressed.

There are various directions in which our research can be further developed. First, the effects of bulk viscosity should be consistently included in future merger simulations. This has not been attempted before and requires a formulation of the relativistic-hydrodynamic equations that is hyperbolic and stable (see Chap. 6 of [44] for the associated challenges). Second, the bulk viscous effects discussed so far may be amplified by nonlinear suprathermal enhancement [30, 52–55] (which to a weaker extent also affects neutrino cooling, see e.g. [52, 56]), or by the even stronger phase-conversion dissipation [57]. Third, because the role played by shear viscosity depends on the typical scale-height of the fluid flow, investigations of the development of turbulent motion in the post-merger phase will be essential. Finally, given the role they play in determining the strength of thermal transport and of shear/bulk dissipation, neutrino trapping and direct-Urca processes motivate additional work to constrain the conditions under which these phenomena occur. We plan to consider some of these topics in our future work.

Acknowledgements. Support comes from: the U.S. Department of Energy, Office of Science, Office of Nuclear Physics under Award Number #DE-FG02-05ER41375; "NewCompStar", COST Action MP1304; LOEWE-Program in HIC for FAIR; European Union's Horizon 2020 Research and Innovation Programme (Grant 671698) (call FETHPC-1-2014, project ExaHyPE). We to thank A. Bauswein, T. Fischer, S. Han, G. McLaughlin, V. Paschalidis, S. Reddy, A. Sedrakian, S. Shapiro, and P. Shternin for very helpful discussions. MGA and KS acknowledge hospitality at the Institute for Theoretical Physics in Frankfurt and at the Institute for Nuclear Theory in Seattle during the program INT-16-2b "The Phases of Dense Matter".

[1] B. P. Abbott, R. Abbott, T. D. Abbott, F. Acernese, K. Ackley, C. Adams, T. Adams, P. Addesso, R. X. Adhikari, V. B. Adya, and et al., Astrophys. J. Lett. **848**, L12 (2017).
[2] B. P. Abbott *et al.* (Virgo, LIGO Scientific), Phys. Rev. Lett. **119**, 161101 (2017), arXiv:1710.05832 [gr-qc] .
[3] B. P. Abbott *et al.* (Virgo, LIGO Scientific), Phys. Rev. Lett. **116**, 061102 (2016), arXiv:1602.03837 [gr-qc] .
[4] L. Baiotti and L. Rezzolla, Reports on Progress in Physics (2016), 10.1088/1361-6633/aa67bb, arXiv:1607.03540 [gr-qc] .
[5] V. Paschalidis, Classical and Quantum Gravity **34**, 084002 (2017), arXiv:1611.01519 [astro-ph.HE] .
[6] M. D. Duez, Y. T. Liu, S. L. Shapiro, and B. C. Stephens, Phys. Rev. **D69**, 104030 (2004), arXiv:astro-ph/0402502 [astro-ph] .
[7] M. Shibata and K. Kiuchi, arXiv:1705.06142 (2017), arXiv:1705.06142 [astro-ph.HE] .
[8] L. Bildsten and C. Cutler, Astrophys. J. **400**, 175 (1992).
[9] M. Shibata and K. Uryū, Phys. Rev. D **61**, 064001 (2000), gr-qc/9911058 .
[10] L. Baiotti, B. Giacomazzo, and L. Rezzolla, Phys. Rev. D **78**, 084033 (2008), arXiv:0804.0594 [gr-qc] .
[11] M. Anderson, E. W. Hirschmann, L. Lehner, S. L. Liebling, P. M. Motl, D. Neilsen, C. Palenzuela, and J. E. Tohline, Phys. Rev. D **77**, 024006 (2008), arXiv:0708.2720 [gr-qc] .
[12] Y. T. Liu, S. L. Shapiro, Z. B. Etienne, and K. Taniguchi, Phys. Rev. D **78**, 024012 (2008), arXiv:0803.4193 [astro-ph] .
[13] S. Bernuzzi, M. Thierfelder, and B. Brügmann, Phys. Rev. D **85**, 104030 (2012), arXiv:1109.3611 [gr-qc] .
[14] A. Bauswein and H.-T. Janka, Phys. Rev. Lett. **108**, 011101 (2012), arXiv:1106.1616 [astro-ph.SR] .
[15] N. Stergioulas, A. Bauswein, K. Zagkouris, and H.-T. Janka, Mon. Not. R. Astron. Soc. **418**, 427 (2011), arXiv:1105.0368 [gr-qc] .
[16] K. Takami, L. Rezzolla, and L. Baiotti, Phys. Rev. Lett. **113**, 091104 (2014), arXiv:1403.5672 [gr-qc] .
[17] S. Bernuzzi, T. Dietrich, and A. Nagar, Phys. Rev. Lett. **115**, 091101 (2015), arXiv:1504.01764 [gr-qc] .
[18] L. Rezzolla and K. Takami, Phys. Rev. D **93**, 124051 (2016), arXiv:1604.00246 [gr-qc] .
[19] K. P. Levenfish and D. G. Yakovlev, Astronomy Reports **38**, 247 (1994).
[20] S. Reddy, M. Prakash, and J. M. Lattimer, Phys. Rev. **D58**, 013009 (1998), arXiv:astro-ph/9710115 [astro-ph] .
[21] P. Shternin and D. Yakovlev, Phys.Rev. **D75**, 103004 (2007), arXiv:0705.1963 [astro-ph] .
[22] L. F. Roberts and S. Reddy, Phys. Rev. **C95**, 045807 (2017), arXiv:1612.02764 [astro-ph.HE] .
[23] B. T. Goodwin and C. J. Pethick, Astrophys. J. **253**, 816 (1982).
[24] P. S. Shternin and D. G. Yakovlev, Phys. Rev. **D78**, 063006 (2008), arXiv:0808.2018 [astro-ph] .
[25] C. Manuel and L. Tolos, Phys. Rev. **D88**, 043001 (2013), arXiv:1212.2075 [astro-ph.SR] .
[26] K. Kiuchi, P. Cerdá-Durán, K. Kyutoku, Y. Sekiguchi, and M. Shibata, Phys. Rev. **D92**, 124034 (2015), arXiv:1509.09205 [astro-ph.HE] .
[27] W. E. East, V. Paschalidis, F. Pretorius, and S. L. Shapiro, Phys. Rev. D **93**, 024011 (2016), arXiv:1511.01093 [astro-ph.HE] .
[28] D. Radice, S. Bernuzzi, and C. D. Ott, Phys. Rev. D **94**, 064011 (2016), arXiv:1603.05726 [gr-qc] .
[29] L. Lehner, S. L. Liebling, C. Palenzuela, and P. M. Motl, Phys. Rev. D **94**, 043003 (2016), arXiv:1605.02369 [gr-qc] .
[30] M. G. Alford, S. Mahmoodifar, and K. Schwenzer, J. Phys. **G37**, 125202 (2010), arXiv:1005.3769 [nucl-th] .
[31] P. Demorest, T. Pennucci, S. Ransom, M. Roberts, and J. Hessels, Nature **467**, 1081 (2010), arXiv:1010.5788 [astro-ph.HE] .
[32] J. Antoniadis, P. C. C. Freire, N. Wex, T. M. Tauris, R. S. Lynch, M. H. van Kerkwijk, M. Kramer, C. Bassa, V. S. Dhillon, T. Driebe, J. W. T. Hessels, V. M. Kaspi, V. I. Kondratiev, N. Langer, T. R. Marsh, M. A. McLaughlin, T. T. Pennucci, S. M. Ransom, I. H. Stairs, J. van Leeuwen, J. P. W. Verbiest, and D. G. Whelan, Science **340**, 448 (2013), arXiv:1304.6875 [astro-ph.HE] .
[33] A. Akmal, V. R. Pandharipande, and D. G. Ravenhall, Phys. Rev. **C58**, 1804 (1998), arXiv:nucl-th/9804027 .
[34] M. Hempel and J. Schaffner-Bielich, Nucl. Phys. **A837**, 210 (2010), arXiv:0911.4073 [nucl-th] .
[35] J. M. Lattimer and F. D. Swesty, Nucl. Phys. **A535**, 331 (1991).
[36] A. W. Steiner, M. Hempel, and T. Fischer, Astrophys. J. **774**, 17 (2013), arXiv:1207.2184 [astro-ph.SR] .

[37] T. Fischer, M. Hempel, I. Sagert, Y. Suwa, and J. Schaffner-Bielich, Eur. Phys. J. **A50**, 46 (2014), arXiv:1307.6190 [astro-ph.HE] .

[38] T. Dietrich and M. Ujevic, Classical and Quantum Gravity **34**, 105014 (2017), arXiv:1612.03665 [gr-qc] .

[39] M. Hanauske, K. Takami, L. Bovard, L. Rezzolla, J. A. Font, F. Galeazzi, and H. Stöcker, Phys. Rev. D **96**, 043004 (2017), arXiv:1611.07152 [gr-qc] .

[40] E. E. Kolomeitsev, J. M. Lattimer, A. Ohnishi, and I. Tews, (2016), arXiv:1611.07133 [nucl-th] .

[41] T. Klahn *et al.*, Phys. Rev. **C74**, 035802 (2006), arXiv:nucl-th/0602038 [nucl-th] .

[42] R. F. Sawyer, Phys. Rev. **D39**, 3804 (1989).

[43] K. Takami, L. Rezzolla, and L. Baiotti, Phys. Rev. D **91**, 064001 (2015), arXiv:1412.3240 [gr-qc] .

[44] L. Rezzolla and O. Zanotti, *Relativistic Hydrodynamics* (Oxford University Press, Oxford, UK, 2013).

[45] L. Bovard and L. Rezzolla, Classical and Quantum Gravity **34**, 215005 (2017), arXiv:1705.07882 .

[46] F. Maione, R. De Pietri, A. Feo, and F. Löffler, arXiv:1707.03368 (2017), arXiv:1707.03368 [gr-qc] .

[47] J. A. Clark, A. Bauswein, N. Stergioulas, and D. Shoemaker, Class. Quantum Grav. **33**, 085003 (2016), arXiv:1509.08522 [astro-ph.HE] .

[48] S. Bose, K. Chakravarti, L. Rezzolla, B. S. Sathyaprakash, and K. Takami, arXiv:1705.10850 (2017), arXiv:1705.10850 [gr-qc] .

[49] Y. Sekiguchi, K. Kiuchi, K. Kyutoku, and M. Shibata, Phys. Rev. Lett. **107**, 051102 (2011), arXiv:1105.2125 [gr-qc] .

[50] V. Paschalidis, Z. B. Etienne, and S. L. Shapiro, Phys. Rev. **D86**, 064032 (2012), arXiv:1208.5487 [astro-ph.HE] .

[51] J. D. Kaplan, C. D. Ott, E. P. O'Connor, K. Kiuchi, L. Roberts, and M. Duez, Astrophys. J. **790**, 19 (2014), arXiv:1306.4034 [astro-ph.HE] .

[52] A. Reisenegger and A. A. Bonacic, (2003), arXiv:astro-ph/0303454 .

[53] A. A. Bonacic, Master thesis, Universidad Catolica de Chile (2003).

[54] M. G. Alford, S. Reddy, and K. Schwenzer, Phys. Rev. Lett. **108**, 111102 (2012), arXiv:1110.6213 [nucl-th] .

[55] M. G. Alford and K. Pangeni, Phys. Rev. **C95**, 015802 (2017), arXiv:1610.08617 [nucl-th] .

[56] M. G. Alford and K. Schwenzer, Astrophys.J. **781**, 26 (2014), arXiv:1210.6091 [gr-qc] .

[57] M. G. Alford, S. Han, and K. Schwenzer, Phys. Rev. **C91**, 055804 (2015), arXiv:1404.5279 [astro-ph.SR] .